DBF-code

Eralp Demir[1]

[1]Department of Engineering Science, University of Oxford

October 2022

Contents

1 Introduction

This is a UMAT code written for crystal plasticity calculations at University of Oxford for DBF project.

This code is rewrite of UMAT by Ed Tarleton and Nicolo Grilli which was based on UEL by Fionn Dunne 2007.

Major changes are:

- Forward-gradient Euler predictor scheme for better convergence
- Option for implicit state update
- Multiple materials with different phases can co-exist in a mesh
- Modular code for flexible constitutive model development
- GND calculations:
  - Multiple options for GND calculation (i.e. curlFp or slip gradients)
  - Option for element center homogenization
  - Different element types for GND calculation
- 2D plane stress/strain problems

Unit system of the code:

2 Crystal plasticity

This section describes the technical part involving the solution of crystal plasticity problem. The outline is as follows:

- 2.1 Crystal plasticity kinematics
- 2.2 Constitutive laws
- 2.3 Explicit state update based on Cauchy stress
- 2.4 Implicit state update

Similar symbols as in the code is used in this document.

2.1 Crystal plasticity kinematics

The total deformation gradient, $\mathbf{F}_{tot}$, consists of mechanical, $\mathbf{F}$, and thermal parts, $\mathbf{F}_{th}$ as in Eq. (2.1). We used the decomposition similar in references [1, 2, 3]. This is schematically shown in Fig. 1.

$$\mathbf{F}_{tot} = \mathbf{F}_e \mathbf{F}_p \mathbf{F}_{th}. \tag{2.1}$$

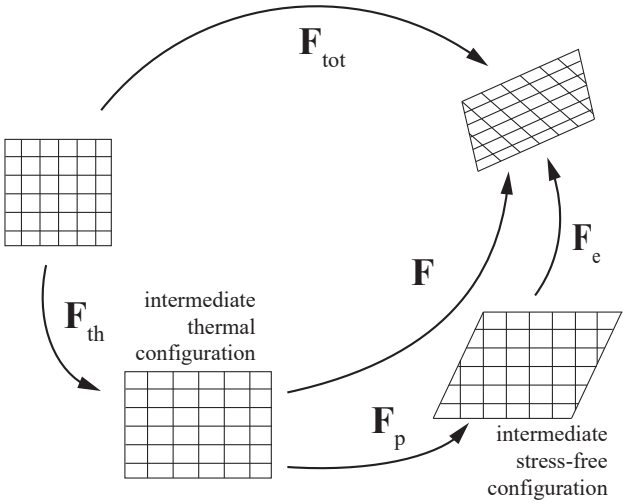

Figure 1: Multiplicative decomposition of total deformation.

The thermal part of the strain increment at the crystal lattice is computed using Eq. (2.2) in which α is the thermal expansion coefficient, ΔT represents the temperature increment, and Δt is the time increment:

$$(\Delta \mathbf{E}_{th})_0 = \alpha \, \Delta T \, \Delta t \tag{2.2}$$

The thermal expansion coefficient is generalized as in Eq. (2.3) in which α_1, α_2, α_3 are the thermal expansion coefficients in the principal cartersian directions in the lattice frame:

$$\alpha = \begin{bmatrix} \alpha_1 & 0 & 0 \\ 0 & \alpha_2 & 0 \\ 0 & 0 & \alpha_3 \end{bmatrix} \tag{2.3}$$

This is then transformed to sample reference using the crystal-to-sample transformation, $\mathbf{g}^T$, using Eq. (2.4):

$$\Delta \mathbf{E}_{th} = \mathbf{g}^T \, (\Delta \mathbf{E}_{th})_0 \, \mathbf{g} \tag{2.4}$$

The thermal deformation gradient initiates with identity matrix $\mathbf{I}$ and computed incrementally using Eq. (2.5):

$$\mathbf{F}_{th} = (\mathbf{F}_{th})_t + \Delta \mathbf{E}_{th} \tag{2.5}$$

Mechanical part of the deformation gradient is computed from Eq. (2.6):

$$\mathbf{F} = \mathbf{F}_{tot} \mathbf{F}_{th}^{-1}. \tag{2.6}$$

Multiplicative decomposition of mechanical deformation into elastic and plastic strains through Eq. (2.7):

$$\mathbf{F} = \mathbf{F}_e \mathbf{F}_p. \tag{2.7}$$

with volume during plastic deformation remaining constant, Eq. (2.8):

$$\det(\mathbf{F}_p) = 1. \tag{2.8}$$

Plastic velocity gradient is the sum of the slip rates in which dyadic product of slip direction and slip plane normal, Schmid tensor, transforms the slip rates from slip system to the deformed crystal reference in Eq. (2.9):

$$\mathbf{L}_p = \sum_a \dot{\gamma}^a \mathbf{s}_e^a \otimes \mathbf{n}_e^a. \tag{2.9}$$

Schmid tensor or dyadic in the deformed configuration, $\mathbf{S}_e^a$, for the slip system a is defined as in Eq. (2.10). Schmid tensor transforms the slip (simple shear) in the slip reference frame that is prescribed by the slip direction, $\mathbf{s}_e^a$, and slip plane normal, $\mathbf{n}_e^a$, to the crystal reference:

$$\mathbf{S}_e^a = \mathbf{s}_e^a \otimes \mathbf{n}_e^a. \tag{2.10}$$

Derivation of Schmid tensor [4]:

Slip is in the form of simple shear, hence the strain in the slip reference,ε^s, is given by Eq. (2.11):

$$\varepsilon^s = \begin{bmatrix} 0 & \gamma & 0 \\ 0 & 0 & 0 \\ 0 & 0 & 0 \end{bmatrix}. \tag{2.11}$$

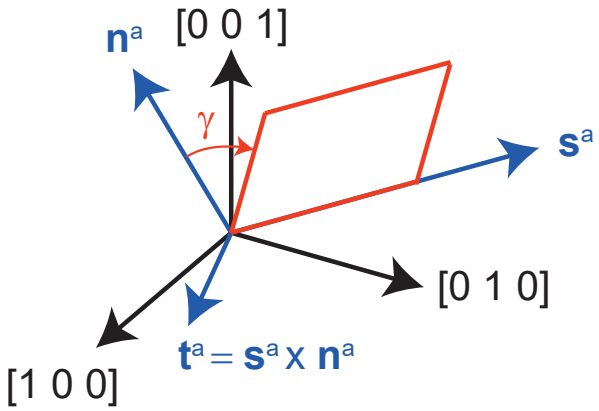

Figure 2: Slip in simple shear form (red color) on slip reference (blue color) and crystal reference (black color).

The transformation from slip reference to the crystal reference in Fig. 2) is given by Eq. (2.12):

$$\mathbf{g}^{s2c} = \begin{bmatrix} \mathbf{s}^a & \mathbf{n}^a & \mathbf{t}^a \end{bmatrix}. \tag{2.12}$$

Note that $\mathbf{g}_{slip2crystal}$ is 3x3 matrix that transforms the slip vector in slip reference to the crystal reference with Eq. (2.13):

$$\mathbf{g}^{s2c} \begin{Bmatrix} 1 \\ 0 \\ 0 \end{Bmatrix} = \begin{bmatrix} \mathbf{s}^a & \mathbf{n}^a & \mathbf{t}^a \end{bmatrix} \begin{Bmatrix} 1 \\ 0 \\ 0 \end{Bmatrix} = \mathbf{s}^a. \tag{2.13}$$

Similarly the slip plane normal in slip reference transforms to the crystal reference according to Eq. (2.14) with $\mathbf{g}_{s2c}$:

$$\mathbf{g}^{s2c} \begin{Bmatrix} 0 \\ 1 \\ 0 \end{Bmatrix} = \begin{bmatrix} \mathbf{s}^a & \mathbf{n}^a & \mathbf{t}^a \end{bmatrix} \begin{Bmatrix} 0 \\ 1 \\ 0 \end{Bmatrix} = \mathbf{n}^a. \tag{2.14}$$

Therefore we can use $\mathbf{g}^{s2c}$ to transform the slip strain on the slip reference to the crystal reference. But this time we strain as a second rank tensor hence transformation has to be applied twice. Using index notation the slip in crystal transforms with Eq. (2.15):

$$\varepsilon^c_{ij} = g^{s2c}_{im}\, \varepsilon^s_{mn}\, g^s 2c_{nj}. \tag{2.15}$$

Since there is only ε^s_{12} term, Eq. (2.16) can be concluded:

$$\varepsilon^c_{ij} = g^{s2c}_{i1}\, \varepsilon^s_{12}\, g^s 2c_{2j}. \tag{2.16}$$

Note that the following identities hold in Eq. (2.17) and Eq. (2.18):

$$g^{s2c}_{i1} = s^a_i. \tag{2.17}$$

$$g^{s2c}_{2j} = n^a_j. \tag{2.18}$$

Substituting these identities, the transformation becomes as in Eq. (2.19) knowing that $\varepsilon^s_{12} = \gamma$:

$$\varepsilon^c_{ij} = s^a_i\, n^a_j\, \gamma. \tag{2.19}$$

$s^a_i\, n^a_j$ represents the dyadic product of the slip direction and slip plane normal vectors which gives the Schmid tensor, Eq. (2.20):

$$S^a_{ij} = s^a_i\, n^a_j = \mathbf{S}^a = \mathbf{s}^a \otimes \mathbf{n}^a. \tag{2.20}$$

Therefore, Schmid tensor is the transformation required to find the correspondent strain at the in the crystal reference due to slip in a slip system.

Eq. (2.21) transforms the slip direction to deformed reference:

$$\mathbf{s}^a_e = \mathbf{F}_e\, \mathbf{s}^a. \tag{2.21}$$

Eq. (2.22) transforms the slip plane normal to deformed reference:

$$\mathbf{n}^a_e = \mathbf{F}_e^{-T}\, \mathbf{n}^a = \mathbf{n}^a\, \mathbf{F}_e^{-1}. \tag{2.22}$$

Derivation of Eq. (2.22):

Slip direction and slip plane normal are perpendicular to each other giving Eq. (2.23):

$$\mathbf{s}^a \cdot \mathbf{n}^a = 0. \tag{2.23}$$

To maintain the equality in Eq. (2.23), let the deformed vectors map with arbitrary $\mathbf{A}$ and $\mathbf{B}$ mappings such that deformed slip direction and slip plane normal become as in Equations (2.24) and (2.25), respectively:

$$\mathbf{s}^a_e = \mathbf{A}\, \mathbf{s}^a. \tag{2.24}$$

$$\mathbf{n}^a_e = \mathbf{B}\, \mathbf{n}^a. \tag{2.25}$$

Substituting Eq. (2.24) and Eq. (2.25) to Eq. (2.23) gives (2.26):

$$(\mathbf{A}\,\mathbf{s}^a) \cdot (\mathbf{B}\,\mathbf{n}^a) = 0 \tag{2.26}$$

The transpose property gives Eq. (2.27):

$$(\mathbf{s}^a\,\mathbf{A}^T) \cdot (\mathbf{B}\,\mathbf{n}^a) = 0. \tag{2.27}$$

Further simplification gives Eq. (2.28):

$$\mathbf{s}^a\,(\mathbf{A}^T \cdot \mathbf{B})\,\mathbf{n}^a = 0. \tag{2.28}$$

In order for Eq. (2.23) to hold, Eq. (2.29) must be satisfied:

$$\mathbf{A}^T \cdot \mathbf{B} = \mathbf{I}. \tag{2.29}$$

giving Eq. (2.30):

$$\mathbf{B} = \mathbf{A}^{-T}. \tag{2.30}$$

Deformation gradient directly map the slip directions giving (2.31):

$$\mathbf{A} = \mathbf{F}_e. \tag{2.31}$$

Therefore, slip planes map with Eq. (2.32):

$$\mathbf{B} = \mathbf{F}_e^{-T}. \tag{2.32}$$

Velocity gradient is given by Eq. (2.33):

$$\mathbf{L} = \dot{\mathbf{F}}\mathbf{F}^{-1}. \tag{2.33}$$

Velocity gradient can be expressed as the sum of symmetric stretch, $\mathbf{D}$, and anti-symmetric spin tensors, Ω, as in Eq. (2.34):

$$\mathbf{L} = \mathbf{D} + \Omega. \tag{2.34}$$

The stretch can be decomposed into its elastic and plastic parts as in Eq. (2.35):

$$\mathbf{D} = \mathbf{D}_e + \mathbf{D}_p. \tag{2.35}$$

similar to spin in Eq. (2.36):

$$\Omega = \Omega_e + \Omega_p. \tag{2.36}$$

Note the elastic velocity gradient in the deformed configuration becomes in Eq. (2.37):

$$\mathbf{L}_e = \Omega_e + \mathbf{D}_e. \tag{2.37}$$

Similarly plastic part of the velocity can be expressed with Eq. (2.38) using Eq. (2.9):

$$\mathbf{L}_p = \Omega_p + \mathbf{D}_p = \sum_a \dot{\gamma}^a \mathbf{s}^a \otimes \mathbf{n}^a. \tag{2.38}$$

2.2 Constitutive laws

Elasticity relates rotation-free objective Jaumann rate of stress to elastic stretch through elasticity as in Eq. (2.39):

$$\overset{\nabla}{\boldsymbol{\sigma}}_e \approx \mathbf{C} : \mathbf{D}_e. \tag{2.39}$$

A more accurate relation is provided with Eq. (2.40) according to Hill and Rice [5]:

$$\overset{\nabla}{\boldsymbol{\sigma}}_e + \boldsymbol{\sigma}(\mathbf{I} : \mathbf{D}_e) = \mathbf{C} : \mathbf{D}_e. \tag{2.40}$$

where $\mathbf{C}$ is the elasticity matrix in the deformed configuration and it is obtained by the transformation of elasticity in the crystal reference to the sample or deformed reference using Eq. (2.41):

$$\mathbf{C} = \mathbf{R}\,\mathbf{C}_0\,\mathbf{R}^T. \tag{2.41}$$

$\mathbf{R}$ is a 6x6 special transformation matrix that is constructed from the crystal to sample tranformation matrix, $\mathbf{g}^T$ as shown in Eq. (2.42) according to the ref. [6].

$$\mathbf{R} = \begin{bmatrix} (g^T_{11})^2 & (g^T_{12})^2 & (g^T_{13})^2 & 2g^T_{11}g^T_{12} & 2g^T_{13}g^T_{11} & 2g^T_{12}g^T_{13} \\ (g^T_{21})^2 & (g^T_{22})^2 & (g^T_{23})^2 & 2g^T_{21}g^T_{22} & 2g^T_{23}g^T_{21} & 2g^T_{22}g^T_{23} \\ (g^T_{31})^2 & (g^T_{32})^2 & (g^T_{33})^2 & 2g^T_{31}g^T_{32} & 2g^T_{33}g^T_{31} & 2g^T_{32}g^T_{33} \\ g^T_{11}g^T_{21} & g^T_{12}g^T_{22} & g^T_{13}g^T_{23} & g^T_{11}g^T_{22}+g^T_{12}g^T_{21} & g^T_{13}g^T_{21}+g^T_{11}g^T_{23} & g^T_{12}g^T_{23}+g^T_{13}g^T_{22} \\ g^T_{31}g^T_{11} & g^T_{32}g^T_{12} & g^T_{33}g^T_{13} & g^T_{11}g^T_{32}+g^T_{12}g^T_{31} & g^T_{13}g^T_{31}+g^T_{11}g^T_{33} & g^T_{12}g^T_{33}+g^T_{13}g^T_{32} \\ g^T_{21}g^T_{31} & g^T_{22}g^T_{32} & g^T_{23}g^T_{33} & g^T_{22}g^T_{31}+g^T_{21}g^T_{32} & g^T_{21}g^T_{33}+g^T_{23}g^T_{31} & g^T_{22}g^T_{33}+g^T_{23}g^T_{32} \end{bmatrix}. \tag{2.42}$$

The elasticity in the crystal reference is given by Eq. (2.43) for a cubic material with three independent elastic constants of C_{11}, C_{12}, and C_{44}:

$$\mathbf{C}_0 = \begin{bmatrix} C_{11} & C_{12} & C_{12} & 0 & 0 & 0 \\ C_{12} & C_{11} & C_{12} & 0 & 0 & 0 \\ C_{12} & C_{12} & C_{11} & 0 & 0 & 0 \\ 0 & 0 & 0 & C_{44} & 0 & 0 \\ 0 & 0 & 0 & 0 & C_{44} & 0 \\ 0 & 0 & 0 & 0 & 0 & C_{44} \end{bmatrix}. \tag{2.43}$$

Similarly, the elasticity in the crystal reference is given by Eq. (2.43) for a hexagonal material with five independent elastic constants of C_{11}, C_{12}, C_{13}, C_{33}, and C_{44}:

$$\mathbf{C}_0 = \begin{bmatrix} C_{11} & C_{12} & C_{13} & 0 & 0 & 0 \\ C_{12} & C_{11} & C_{13} & 0 & 0 & 0 \\ C_{13} & C_{13} & C_{33} & 0 & 0 & 0 \\ 0 & 0 & 0 & C_{44} & 0 & 0 \\ 0 & 0 & 0 & 0 & C_{44} & 0 \\ 0 & 0 & 0 & 0 & 0 & \dfrac{C_{11}-C_{12}}{2} \end{bmatrix}. \tag{2.44}$$

Initial (undeformed) sample to crystal transformation matrix, $\mathbf{g}_0$, is computed using the Euler angles (Bunge convention) as in Eq. (2.45). ϕ_1, Φ, and ϕ_2 represent the rotation angles about Z, rotated X', and rotated-rotated Z" axes, respectively. Alternative definitions for this transformation can be found.

$$\mathbf{g}_0 = \begin{bmatrix} \cos\phi_1\cos\phi_2 - \sin\phi_1\sin\phi_2\cos\Phi & \sin\phi_1\cos\phi_2 - \cos\phi_1\sin\phi_2\cos\Phi & \sin\phi_2\sin\Phi \\ -\cos\phi_1\sin\phi_2 - \sin\phi_1\cos\phi_2\cos\Phi & -\sin\phi_1\sin\phi_2 + \cos\phi_1\cos\phi_2\cos\Phi & \cos\phi_2\sin\Phi \\ \sin\phi_1\sin\Phi & -\cos\varphi_1\sin\Phi & \cos\Phi \end{bmatrix} \quad (2.45)$$

2.3 Explicit method

This method is based on the crystal plasticity solution method explained in the reference [7].

The formulation is based on deformed vectors. The stress at the deformed configuration, Cauchy stress, is given by Eq. (2.46) in which $\mathbf{C}$ is the elasiticity in the deformed configuration given by Eq. (2.41):

$$\sigma = \mathbf{C} : \varepsilon_e. \quad (2.46)$$

The elastic strain is obtained by summing up the former elastic strain with the elastic strain increment as in Eq. (2.47):

$$\varepsilon_e = \varepsilon_e(t) + \Delta\varepsilon_e. \quad (2.47)$$

The elastic strain increment can further be represented as the total strain increment minus the plastic strain increment in Eq. (2.48):

$$\Delta\varepsilon_e = \Delta\varepsilon - \Delta\varepsilon_p. \quad (2.48)$$

Substituting gives the trial stress and corrector scheme in Eq. (2.49):

$$\sigma = \mathbf{C} : (\varepsilon_e(t) + \Delta\varepsilon) - \mathbf{C} : \Delta\varepsilon_p. \quad (2.49)$$

The residual, ψ, that will be minimized by Newton-Raphson method, is Cauchy stress Eq. (2.50):

$$\psi = \sigma - \sigma_{tr} + \mathbf{C} : \Delta\varepsilon_p = \mathbf{0}. \quad (2.50)$$

The plastic strain increment is the sum of the slip increments in the deformed reference, but considering the stretch (symmetric) part of the velocity gradient giving Eq. (2.51):

$$\Delta\varepsilon_p = \mathrm{sym}\left(\sum_a \dot{\gamma}^a \mathbf{S}^a\right)\Delta t. \quad (2.51)$$

Differentiation of the residual with respect to the Cauchy stress gives Eq. (2.52):

$$\frac{\partial\psi}{\partial\sigma} = \mathbf{I} + \mathbf{C}\mathbf{P}. \quad (2.52)$$

where $\mathbf{P}$ is obtained by differentiating $\Delta\varepsilon_p$ with respect to σ and using chain-rule of differentiation as in Eq. (2.53):

$$\mathbf{P} = \frac{\partial\sum_a \dot{\gamma}^a \mathbf{S}^a}{\partial\sigma}\Delta t = \sum_a \frac{\partial\dot{\gamma}^a}{\partial\tau^a}\mathbf{S}^a\frac{\partial\tau^a}{\partial\sigma}\Delta t. \quad (2.53)$$

Note the derivative of resolved shear stress with respect to the stress is simply the Schmid tensor, Eq. (2.54):

$$\frac{\partial\tau^a}{\partial\sigma} = \mathbf{S}^a. \quad (2.54)$$

Substituting Eq. (2.54) to Eq. (2.53) gives the expression for the $\mathbf{P}$ matrix in Eq. (2.55):

$$\mathbf{P} = \Delta t \sum_a \frac{\partial \dot{\gamma}^a}{\partial \tau^a} \mathbf{S}^a \otimes \mathbf{S}^a. \tag{2.55}$$

Newton-Raphson solution involves the function value and its derivative to obtain a new solution. Applying this to the residual and its derivative gives the stress increment as in Eq. (2.56):

$$\Delta\sigma = -\left[\frac{\partial \psi}{\partial \sigma}\right]^{-1} \{\psi\}. \tag{2.56}$$

Substituting Eq. (2.50) and Eq. (2.52) to Eq. (2.56), gives the expression for the stress increment, Eq. (2.57):

$$\Delta\sigma = -\left[\mathbf{I} + \mathbf{C} : \mathbf{P}\right]^{-1} \left\{\sigma - \sigma_{tr} + \mathbf{C} : \Delta t \sum_a \frac{\partial \dot{\gamma}^a}{\partial \tau^a} \mathbf{S}^a \otimes \mathbf{S}^a\right\}. \tag{2.57}$$

Therefore, the stress is updated using Eq. (2.58) until the increments gets smaller than a tolerance:

$$\begin{aligned} \sigma^{k+1} &= \sigma^k + \Delta\sigma^k, \\ \|\Delta\sigma\| &< 10^{-8}\,\text{MPa}. \end{aligned} \tag{2.58}$$

Note that the initial guess for the solver is also very important since "Newton-Raphson method converges iff there is a good guess!". The initial guess is obtained by a weighted average of the fully-elastic ($\sigma_t r$) and fully-plastic ($\sigma(t)$) guesses as in Eq. (2.59):

$$\sigma^0 = (1 - \phi)\,\sigma_{tr} + \phi\,\sigma(t). \tag{2.59}$$

Once the slip rates are computed, the corresponding states (hardening or softening) are updated explicitly.

2.3.1 Material tangent

Material tangent is simply the derivative of stress increment with respect to the total strain increment, Eq. (2.60). It does not have an effect on the accuracy of the solution but it determines the rate of convergence:

$$\frac{\partial \sigma}{\partial \Delta\varepsilon}. \tag{2.60}$$

Taking the variation of stress increment in Eq. (2.50) gives Eq. (2.61):

$$\partial\sigma - \partial\sigma_{tr} + \mathbf{C} : \partial\Delta\varepsilon_p = \mathbf{0}. \tag{2.61}$$

The variation of trial stress becomes, Eq. (2.62):

$$\partial\sigma_{tr} = \mathbf{C} : \partial[\varepsilon_e(t) + \Delta\varepsilon] = \mathbf{C} : \partial\Delta\varepsilon. \tag{2.62}$$

The variation of plastic strain increment becomes, Eq. (2.63):

$$\partial\Delta\varepsilon_p = \mathbf{C}\mathbf{P}\partial\sigma. \tag{2.63}$$

Substituting Eq. (2.62) and Eq. (2.63) to Eq. (2.61) gives Eq. (2.64):

$$\partial\sigma - \mathbf{C} : \partial\Delta\varepsilon + \mathbf{C}\mathbf{P}\partial\sigma = \mathbf{0}. \tag{2.64}$$

Re-arranging terms reveals Eq. (2.65) for the material tangent:

$$\frac{\partial \sigma}{\partial \Delta\varepsilon} = \left[\mathbf{I} + \mathbf{C}\mathbf{P}\right]^{-1} \mathbf{C}. \tag{2.65}$$

2.4 Implicit method

The implicit integration method is similar to the explicit except the calculation of states are performed within a second loop. When the state variable increment exceeds the tolerance, states are updated and stress solution is performed again. This gives rise to avoid the jumps in the stress-strain curve in the case of strain hardening or softening.

After stress calculation converges, slip rates can be obtained. With those slip rates, the increment of state variables, i.e. τ_c^a, is calculated using Eq. (2.66):

$$\Delta\tau_c^a = \mathbf{h}_b^a |\dot{\gamma}^b| \Delta t. \tag{2.66}$$

and the states are are updated according to Euler integration with Eq. (2.67):

$$(\tau_c^a)^{l+1} = (\tau_c^a)^l + (\Delta\tau_c^a)^l \tag{2.67}$$

The outer loop iteration convergences when Eq. (2.68) is fulfilled:

$$\Delta\tau_c^a < \text{tol}. \tag{2.68}$$

A similar example implicit (semi-implicit) method can be found in the reference [8].

3 Slip models

3.1 sinh law

$$\dot{\gamma}^a = \widetilde{\alpha} \sinh \widetilde{\beta} \left(|\tau^a| - \tau_c^a \right) \operatorname{sgn}(\tau^a) \tag{3.1}$$

if the material is in HCP phase

$$\widetilde{\alpha} = (\frac{c}{a})^2 \alpha \tag{3.2}$$

$$\widetilde{\beta} = (\frac{c}{a})^2 \beta \tag{3.3}$$

else

$$\widetilde{\alpha} = \alpha \tag{3.4}$$

$$\widetilde{\beta} = \beta \tag{3.5}$$

Calculation of α:
if a constant value for α is defined, $\alpha_0 \neq 0$

$$\alpha = \alpha_0 \tag{3.6}$$

else

$$\alpha^a = \rho_m (b^a)^2 \nu_0 \exp\left(-\frac{\Delta F^a}{K_B T} \right) \tag{3.7}$$

$$\rho_m = \psi \rho_m^0 \tag{3.8}$$

*Irradiation alters the fraction of mobile dislocations by the factor ψ.

Calculation of β:
if a constant value for β is defined, $\beta_0 \neq 0$

$$\beta^a = \beta_0 \tag{3.9}$$

else

for a general case with state variables per slip system, ^{a}

$$\beta^a = \frac{\Delta V^a}{K_B T} \tag{3.10}$$

Calculation of ΔV^a:
if a constant multiplier of ΔV_0 for the activation volume is defined, $\Delta V_0 \neq 0$

$$\Delta V^a = \Delta V_0 (b^a)^3 \tag{3.11}$$

else[1]

$$\Delta V^a = \gamma_0 \lambda^a (b^a)^2 \tag{3.12}$$

$$\lambda^a = \frac{1}{\sqrt{\rho_{for}^a}} \tag{3.13}$$

[1] In this case, the initial dislocation density (SSD density) shall have a non-zero value in order to end up with non-zero values for the activation volume and hence slip.

Model parameters:

parameter	definition	unit	variable
α_0	constant value	1/s	slipparam(1)
β_0	constant value	1/MPa	slipparam(2)
ψ	fraction of mobile dislocations	-	slipparam(3)
ρ_m^0	reference mobile dislocation density	$1/\mu\mathrm{m}^2$	slipparam(4)
ΔF	activation energy for slip	J	slipparam(5)
ν_0	attempt frequency	1/s	slipparam(6)
γ_0	scaling factor for the jump distance ($\times$ Burgers vector)	-	slipparam(7)
ΔV_0	factor for activation volume ($\times\ b^3$)	-	slipparam(8)

Ex. To obtain constant α of 0.2 and constant β of 0.3, we can use the following values for model parameters:

parameter	value	unit	variable
α_0	0.2	1/s	slipparam(1)
β_0	0.3	1/MPa	slipparam(2)
ψ	0	-	slipparam(3)
ρ_m^0	0	$1/\mu\mathrm{m}^2$	slipparam(4)
ΔF	0	J	slipparam(5)
ν_0	0	1/s	slipparam(6)
γ_0	0	-	slipparam(7)
ΔV	0	$\mu\mathrm{m}^3$	slipparam(8)

3.2 double exponent law

$$\dot{\gamma}^a = \dot{\gamma}_0 \exp\left\{-\frac{\Delta F}{K_B T}\left[1-\left(\frac{|\tau^a|}{\tau_c^a}\right)^p\right]^q\right\}\mathrm{sgn}(\tau^a) \tag{3.14}$$

Model parameters:

parameter	definition	unit	variable
$\dot{\gamma}_0$	reference slip rate	1/s	slipparam(1)
p	inner exponent	-	slipparam(2)
q	outer exponent	-	slipparam(3)
ΔF_{oct}	activation energy for octahedral slip	J	slipparam(4)
ΔF_{cub}	activation energy for cubic slip	J	slipparam(5)

3.3 power law

$$\dot{\gamma}^a = \dot{\gamma}_0 \left(\frac{|\tau^a|}{\tau_c^a}\right)^n \mathrm{sgn}(\tau^a) \tag{3.15}$$

in which

$$n = n_0 + \frac{\partial n}{\partial T} T \tag{3.16}$$

Model parameters:

parameter	definition	unit	variable
$\dot{\gamma}_0$	reference slip rate	1/s	slipparam(1)
n_0	constant exponent	-	slipparam(2)
$\frac{\partial n}{\partial T}$	slope of exponent wrto temperature	1/K	slipparam(3)

4 Creep models

4.1 model-1

$$\dot{\gamma}^a = \dot{\gamma}_C \exp\left(b_C\,|\tau^a| - \frac{Q_C}{RT}\right)\mathrm{sign}\,(\tau^a) + |\Gamma^a|\,\dot{\gamma}_D \exp\left(b_D\,|\tau^a| - \frac{Q_D}{RT}\right)\mathrm{sign}\,(\tau^a) \tag{4.1}$$

$$\Gamma^a = \int_0^t \dot{\gamma}^a \mathrm{d}t \tag{4.2}$$

Model parameters:

parameter	definition	unit	variable
$\dot{\gamma}_C$	reference creep rate	1/s	creepparam(1)
b_C	creep stress multiplier	1/MPa	creepparam(2)
Q_C	activation energy for creep	J/mol	creepparam(3)
$\dot{\gamma}_D$	reference damage rate	1/s	creepparam(4)
b_D	damage stress multiplier	1/MPa	creepparam(5)
Q_D	activation energy for damage	J/mol	creepparam(6)

5 Irradiation models

5.1 model-1

Irradiation increases the flow stress

$$\tau_c^a = (\tau_c^a)_0 + \tau_s \tag{5.1}$$

which decays with slip strain

$$\tau_s = (\tau_s)_0 \exp\left(-\frac{\Gamma}{\gamma_s}\right) \tag{5.2}$$

where Γ represents the cumulative slip over time and over slip systems.

$$\Gamma^a = \int_0^t \dot{\gamma}^a \mathrm{d}t \tag{5.3}$$

with

$$\Gamma = \sum_a \Gamma^a \tag{5.4}$$

Fraction of mobile dislocation gets less (app. 50%) for irradiated materials.

$$\rho_m = \psi_{irr}\, \rho_m^0 \tag{5.5}$$

Model parameters:

parameter	**definition**	**unit**	**variable**
$(\tau_s)_0$	initial value of solute strength	MPa	irradiationparam(1)
γ_s	saturation value of slip strain	-	irradiationparam(2)
ψ_{irr}	fraction of mobile dislocations	-	irradiationparam(3)

5.2 model-2

The irradiation slip resistance is computed with number density of dislocation loops per volume, N_i, and the average diameter of these loops, d_i from reference [9]:

$$\tau_{loop} = G b^a \sqrt{\sum_i (S_i^a)^2 N_i d_i} \tag{5.6}$$

The areal density of loops is used as the state variable. Three different defect populations are active in the model ($i = 1, 2, 3$):

$$(\rho_{loop})_i = N_i d_i \tag{5.7}$$

H_i^a is a matrix that describes the obstacle strengths for different type of defects. It is defined as a 30 by 3 matrix for HCP material directly.

The evolution of loop density is governed by the ODE in which H_i^a represents the softening (hardening) interactions between the defects and slip systems:

$$(\dot{\rho}_{loop})_i = \sum_a H_i^a \sqrt{(\rho_{loop})_i} \frac{|\dot{\gamma}^a|}{b^a} \tag{5.8}$$

Model parameters:

parameter	**definition**	**unit**	**variable**
n	total number of different types of defects	-	irradiationparam(1)
N_1	initial number density of type-1 defects	$1/\mu\text{m}^3$	irradiationparam(2)
$\vdots$	$\vdots$	$\vdots$	$\vdots$
N_n	initial number density of type-n defects	$1/\mu\text{m}^3$	irradiationparam(n+1)
d_1	diameter of type-1 defects	μm	irradiationparam(n+2)
$\vdots$	$\vdots$	$\vdots$	$\vdots$
d_n	diameter of type-n defects	μm	irradiationparam(2*n+2)
$\mathbf{r}_1$	cryst. direction of type-1 defects	-	irradiationparam(2n+3)
$\vdots$	$\vdots$	$\vdots$	$\vdots$
$\mathbf{r}_n$	cryst. direction of type-n defects	-	irradiationparam(3*n+3)
as_1	strength int. coeff. when $a > 0$	-	irradiationparam(3*n+4)
as_2	strength int. coeff. when $a = 0$	-	irradiationparam(3*n+5)
ah_1	hardening int. coeff. when $a > 0$	-	irradiationparam(3*n+6)
ah_2	hardening int. coeff. when $a = 0$	-	irradiationparam(3*n+7)

6 CRSS

6.1 bcc / fcc / hcp

Overall strength relation is a function of initial slip resistance which is a fraction of $(1-X)$ friction stress, impenetrable obstacle strength (the first term in the square root), forest density (ρ^a_{for}) with geometric factor of ζ, and strength related with the irradiation (r^a_i - irradiationmodel=2) with a different types of defect represented with the subscript i. There is a separate model to account for irradiation resistance using solute strength (τ_s - irradiationmodel=1). Note the superscript a stands for the slip system:

The overall strength relation is a function of initial slip resistance (τ^0_c) and forest dislocation density (ρ^a_{for}) with geometric factor of ζ. Two alternative irradiation models are available. Irradiation model-2, the crss related with the type of defect represented with the subscript i. Alternatively, Irradiation model-1 accounts for irradiation resistance using solute strength (τ_s). The superscript a represents the slip system:

$$\tau^a_c = \underbrace{\tau^0_c}_{\text{initial crss}} + Gb^a \sqrt{\underbrace{\zeta^2 \rho^a_{for}}_{\text{cut-through}} + \underbrace{\sum_i (S^a_i)^2 \rho^a_{loop,i}}_{\text{irr. model-2}}} + \underbrace{\tau_s}_{\text{irr. model-1}} \tag{6.1}$$

Cut-through strength is obtained by forest dislocations which is obtained by the projection of total dislocations:

$$\rho^a_{for} = \xi^a_b \rho^b_{tot} \tag{6.2}$$

ξ^a_b is the forest projection of a dislocation with line direction, $\mathbf{t}^b$ onto a slip system with slip plane normal $\mathbf{n}^a$.

$$\xi^a_b = \left| \mathbf{n}^a \cdot \mathbf{t}^b \right| \tag{6.3}$$

Total dislocation density is the sum of SSD and GND densities:

$$\rho^a_{tot} = \rho^a_{SSD} + \rho^a_{GND} \tag{6.4}$$

6.2 α-uranium

User-defined

7 Strain hardening

Important Note: Initial values of the state variables are assumed to be zero. The initial dislocation density and its effect is taken care within the crss definition $(\tau_c^a)^0$ that exists for all materials.

7.1 no hardening (hardeningmodel=0)

Valid for all phases except alpha-uranium

Only the effect of solute hardening will be considered in the presence of irradiation

$$\Delta\rho_{SSD}^a = 0 \tag{7.1}$$

$$\Delta\tau_c^a = 0 \tag{7.2}$$

Forest dislocations are computed using proper projections (assuming that GND calculation is ON.)

$$\rho_{for}^a = \sum_b \left|\mathbf{n}^a \cdot \mathbf{t}_e^b\right| \rho_{GND,e}^b + \left|\mathbf{n}^a \cdot \mathbf{s}_s^b\right| \rho_{GND,s}^b \tag{7.3}$$

Total density is computed based on GNDs (assuming that GND calculation is ON.)

$$\rho_{tot}^a = \sqrt{(\rho_{GND,e}^a)^2 + (\rho_{GND,s}^a)^2} \tag{7.4}$$

$$\Delta\rho_{tot} = \sum_a \rho_{tot}^a \tag{7.5}$$

7.2 Voce type hardening (hardeningmodel=1)

State variable: τ_c^a

$$\Delta\tau_c^a = \sum_b \mathbf{H}_b^a \Delta h^b \tag{7.6}$$

$$\Delta h^b = h_0 \left(1 - \frac{\tau_c^b}{s_s}\right)^m \left|\dot{\gamma}^b\right| \Delta t \tag{7.7}$$

Model parameters:

parameter	definition	unit	variable
h_0	hardening rate	MPa	hardeningparam(1)
s_s	saturation slip strength	MPa	hardeningparam(2)
m	hardening exponent	-	hardeningparam(3)
q	latent hardening exponent	-	hardeningparam(4)

Forest dislocations are computed using proper projections (assuming that GND calculation is ON.)

$$\rho_{for}^a = \sum_b \left|\mathbf{n}^a \cdot \mathbf{t}_e^b\right| \left|\rho_{GND,e}^b\right| + \left|\mathbf{n}^a \cdot \mathbf{s}_s^b\right| \left|\rho_{GND,s}^b\right| \tag{7.8}$$

Total density is computed based on GNDs (assuming that GND calculation is ON.)

$$\rho_{tot}^a = \sqrt{(\rho_{GND,e}^a)^2 + (\rho_{GND,s}^a)^2} \tag{7.9}$$

$$\Delta\rho_{tot} = \sum_a \rho_{tot}^a \tag{7.10}$$

7.3 Linear hardening (hardeningmodel=2)

Per slip system value

$$\Delta\rho^a_{SSD} = k\,|\dot{\gamma}^a|\,\Delta t \tag{7.11}$$

Total value based on Von-Mises equivalent strain rate, $\dot{p}$

$$\Delta\rho_{SSD} = k\,\dot{p}\,\Delta t \tag{7.12}$$

Model parameter:

parameter	definition	unit	variable
k	linear hardening rate	$1/\mu\mathrm{m}^2$	hardeningparam(1)

Forest dislocations are computed using proper projections (assuming that GND calculation is ON.)

$$\rho^a_{for} = \sum_b \left|\mathbf{n}^a \cdot \mathbf{t}^b_e\right| \left|\rho^b_{GND,e} + \rho^b_{SSD,e}\right| + \left|\mathbf{n}^a \cdot \mathbf{s}^b_s\right| \left|\rho^b_{GND,s} + \rho^b_{SSD,s}\right| \tag{7.13}$$

The edge and screw components from SSD density is computed using a proper mapping, χ, that maps the slip system densities into edge and screw families:

$$\left\{ \begin{array}{c} \rho_{SSD,e} \\ \rho_{SSD,s} \end{array} \right\} = [\chi]\,\{\rho_{SSD}\} \tag{7.14}$$

Total density is computed based on GNDs (assuming that GND calculation is ON.)

$$\rho^a_{tot} = \sqrt{(\rho^a_{GND,e})^2 + (\rho^a_{GND,s})^2 + (\rho^a_{SSD})^2} \tag{7.15}$$

$$\rho_{tot} = \rho_{SSD} + \sum_a \sqrt{(\rho^a_{GND,e})^2 + (\rho^a_{GND,s})^2} \tag{7.16}$$

7.4 Kocks-Mecking hardening (hardeningmodel=3)

Per slip system evolution for SSD density

$$\Delta\rho^a_{SSD} = \left(k_1\sqrt{\rho^a_{for}} - k_2(\dot{\varepsilon},T)\,\rho^a_{SSD}\right)|\dot{\gamma}^a|\,\Delta t \tag{7.17}$$

The annihilation constant is computed using

$$k_2 = k_1\frac{\zeta\, b^a}{g^a}\left(1 - \frac{K_B\,T}{D^a\,(b^a)^3}\ln\frac{\dot{\varepsilon}}{\dot{\varepsilon}_0}\right) \tag{7.18}$$

Total value for SSD density

$$\Delta\rho_{SSD} = \sum_a \Delta\rho^a_{SSD} \tag{7.19}$$

Model parameters:

parameter	definition	unit	ex. value	variable
k_1	hardening constant	$1/\mu$m	200	hardeningparam(1)
ζ	dislocation interaction parameter	-	0.9	hardeningparam(2)
g^a	effective activation enthalpy	-	1.5×10^{-3}	hardeningparam(3)
D^a	drag stress	MPa	300	hardeningparam(4)
$\dot{\varepsilon}_0$	reference slip rate	1/s	10^7	hardeningparam(5)

Forest dislocations are computed using proper projections (assuming that GND calculation is ON.)

$$\rho^a_{for} = \sum_b \left|\mathbf{n}^a\cdot\mathbf{t}^b_e\right|\left|\rho^b_{GND,e}+\rho^b_{SSD,e}\right| + \left|\mathbf{n}^a\cdot\mathbf{s}^b_s\right|\left|\rho^b_{GND,s}+\rho^b_{SSD,s}\right| \tag{7.20}$$

The edge and screw components from SSD density is computed using a proper mapping, χ, that maps the slip system densities into edge and screw families:

$$\left\{\begin{array}{c}\rho_{SSD,e}\\ \rho_{SSD,s}\end{array}\right\} = [\chi]\,\{\rho_{SSD}\} \tag{7.21}$$

Total density is computed based on GNDs (assuming that GND calculation is ON.)

$$\rho^a_{tot} = \sqrt{(\rho^a_{GND,e})^2 + (\rho^a_{GND,s})^2 + (\rho^a_{SSD})^2} \tag{7.22}$$

$$\rho_{tot} = \rho_{SSD} + \sum_a \sqrt{(\rho^a_{GND,e})^2 + (\rho^a_{GND,s})^2} \tag{7.23}$$

7.5 Kocks-Mecking hardening with substructure (hardeningmodel=4)

Per slip system evolution for forest density

$$\Delta\rho^a_{for} = \left(k_1\sqrt{\rho^a_{for}} - k_2(\dot{\varepsilon},T)\,\rho^a_{for}\right)|\dot{\gamma}^a|\,\Delta t \tag{7.24}$$

The annihilation constant is computed using

$$k_2 = k_1\frac{X\,b^a}{g^a}\left(1 - \frac{K_B\,T}{D^a\,(b^a)^3}\ln\frac{\dot{\varepsilon}}{\dot{\varepsilon}_0}\right) \tag{7.25}$$

Forest strength;

$$\tau^a_{for} = \zeta\,G^a\,b^a\sqrt{\rho^a_{for}} \tag{7.26}$$

Evolution for substructure density

$$\Delta\rho_{sub} = q\sum_a f^a\sqrt{\rho_{sub}}\,k_2\,\rho^a_{for}\,|\dot{\gamma}^a|\,\Delta t \tag{7.27}$$

Substructure strength;

$$\tau_{sub} = k_{sub}\,G^a\,b^a\sqrt{\rho_{sub}}\log\left(\frac{1}{b^a\sqrt{\rho_{sub}}}\right) \tag{7.28}$$

Overall strength;

$$\tau^a_c = (\tau^a_c)^0 + \tau^a_{for} + \tau_{sub} \tag{7.29}$$

Model parameters:

parameter	definition	unit	ex. value	variable
k_1	hardening constant	$1/\mu$m	200	hardeningparam(1)
ζ	dislocation interaction parameter	-	0.9	hardeningparam(2)
g^a	effective activation enthalpy	-	1.5×10^{-3}	hardeningparam(3)
D^a	drag stress	MPa	300	hardeningparam(4)
$\dot{\varepsilon}_0$	reference slip rate	1/s	10^7	hardeningparam(5)
q	rate coefficient	-	4	hardeningparam(6)
f^a	fraction of recovery rate	-	450	hardeningparam(7)
k_{sub}	empirical parameter	-	0.086	hardeningparam(8)

Forest dislocations are computed using proper projections (assuming that GND calculation is ON.)

$$\rho^a_{for} = \rho^a_{for} + \sum_b \left|\mathbf{n}^a\cdot\mathbf{t}^b_e\right|\rho^b_{GND,e} + \left|\mathbf{n}^a\cdot\mathbf{s}^b_s\right|\rho^b_{GND,s}$$

Total density is computed based on GNDs (assuming that GND calculation is ON.)

$$\rho^a_{tot} = \rho_{sub} + \sqrt{(\rho^a_{GND,e})^2 + (\rho^a_{GND,s})^2} \tag{7.30}$$

$$\rho_{tot} = \rho_{sub} + \sum_a\sqrt{(\rho^a_{GND,e})^2 + (\rho^a_{GND,s})^2} \tag{7.31}$$

Note: The same model was used for alpha-uranium (phase-id = 4, material-id = 9). The hardening parameters however were defined by built-in constants for alpha-uranium only.

8 Strain gradients

There are three different parameters that must set before the GND calculations. Those are listed in the below:

1. **gndmodel**: Strain gradients can be computed by five different methods which are presented as option into the model. There are four different options which are explained in the below.
2. **gndhomogenization**: This parameter determines whether the GNDs will be calculated at each integration point of an element separately (gndhomogenization=0) or, they will be computed justat the centroid of the elements (gndhomogenization=1) assuming the same value for the integation points.
3. **gndlinear**: This parameters determines whether the linear (gndlinear=1) or quadratic (gndlinear=0)interpolation functions will be used for the calculation of strain gradients. This parameter is **ONLY** valid for quadratic elements.

8.1 Derivation of GND calculation

8.1.1 Burgers circuit

Burgers circut is used to get the lattice incompatibility as net Burger vector. For that, a counterclockwise loop is constructed around any arbirtray area normal **r** for the lattice. Net amount of incompatibility is the amount of loop disclosure. This is shown for screw and edge type of dislocations in Fig. 3.

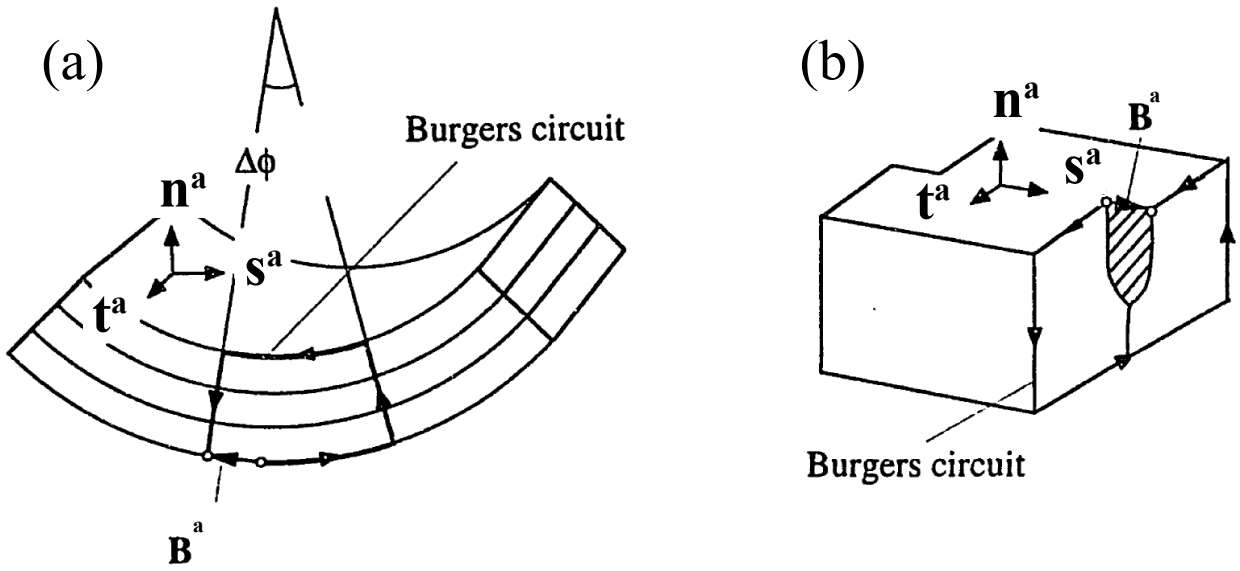

Figure 3: Construction of Burgers circuit around (a) edge and (b) screw type of dislocations. Taken from reference [10].

Net amount of lattice incompatibility for both cases in Fig. 3:

$$\left|OO'\right| = \mathbf{B}_{net} \tag{8.1}$$

For a deformed lattice in terms of the deformed vectors, $\mathbf{Y}$, Burgers circuit on the deformed lattice, C', gives the closure failure as:

$$\mathbf{B}_{net} = -\oint_{C'} \mathrm{d}\mathbf{Y} \tag{8.2}$$

In terms of the undeformed vectors, this expression reduces to a loop around the underformed lattice, C, in terms of the undeformed vectors, $\mathbf{X}$:

$$\mathbf{B}_{net} = -\oint_C \mathbf{F}_p \, \mathrm{d}\mathbf{X} \tag{8.3}$$

since

$$\mathrm{d}\mathbf{Y} = \mathbf{F}_p \, \mathrm{d}\mathbf{X} \tag{8.4}$$

Using Stokes theorem, line integral is converted to curl as in Eq. (8.5). The transpose will be explained in Section 8.1.6.

$$\mathbf{B}_{net} = -\int_S (\nabla \times \mathbf{F}_p)^T \cdot \mathbf{r} \mathrm{d}S \tag{8.5}$$

8.1.2 Curl of a second rank tensor

The curl of a second rank tensor is given in two different references:

- Research paper [11], page 1545
- Wikipedia link: `https://en.wikipedia.org/wiki/Tensor_derivative_(continuum_mechanics)`

For all constant vectors, $\mathbf{c}$:

According to research paper [11]:

$$(\nabla \times \mathbf{A}) \cdot \mathbf{c} = \nabla \times (\mathbf{A}^T \cdot \mathbf{c}) \tag{8.6}$$

$$\nabla \times (\mathbf{A}^T \cdot \mathbf{c}) = \nabla \times (A_{ij} \hat{\mathbf{e}}_j \otimes \hat{\mathbf{e}}_i \cdot c_m \hat{\mathbf{e}}_m) \tag{8.7}$$

$$\nabla \times (\mathbf{A}^T \cdot \mathbf{c}) = \nabla \times (c_i A_{ij} \hat{\mathbf{e}}_j) \tag{8.8}$$

$$\nabla \times (\mathbf{A}^T \cdot \mathbf{c}) = \frac{\partial}{\partial X_k} \hat{\mathbf{e}}_k \times (c_i A_{ij} \hat{\mathbf{e}}_j) \tag{8.9}$$

$$\nabla \times (\mathbf{A}^T \cdot \mathbf{c}) = \varepsilon_{qkj} c_i A_{ij,k} \hat{\mathbf{e}}_q \tag{8.10}$$

$$\nabla \times (\mathbf{A}^T \cdot \mathbf{c}) = (\varepsilon_{qkj} A_{ij,k} \hat{\mathbf{e}}_q \otimes \hat{\mathbf{e}}_i) \cdot c_m \hat{\mathbf{e}}_m = (\nabla \times \mathbf{A}) \cdot \mathbf{c} \tag{8.11}$$

$$(\nabla \times \mathbf{A})_{qi} = \varepsilon_{qkj} A_{ij,k} \hat{\mathbf{e}}_q \otimes \hat{\mathbf{e}}_i \tag{8.12}$$

Or more simply:

$$(\nabla \times \mathbf{A})_{qi} = \varepsilon_{qkj} A_{ij,k} \tag{8.13}$$

The result is obtained as in the reference [11], by just changing the symbols used for the indices ($q \to i$, $i \to j$, $j \to s$, and $k \to r$):

$$(\nabla \times \mathbf{A})_{ij} = \varepsilon_{irs} A_{js,r} \tag{8.14}$$

According to Wikipedia:

$$(\nabla \times \mathbf{T}) \cdot \mathbf{c} = \nabla \times (\mathbf{c} \cdot \mathbf{T}) \tag{8.15}$$

This is indeed using the property of transpose:

$$(\nabla \times \mathbf{T}) \cdot \mathbf{c} = \nabla \times (\mathbf{T}^T \cdot \mathbf{c}) \tag{8.16}$$

Both methods are consistent, revealing the curl of a second rank tensor as:

$$(\nabla \times \mathbf{T})_{km} = \varepsilon_{ijk} T_{mj,i} \hat{\mathbf{e}}_k \otimes \hat{\mathbf{e}}_m \tag{8.17}$$

Or more simply:

$$(\nabla \times \mathbf{T})_{km} = \varepsilon_{ijk} T_{mj,i} \tag{8.18}$$

8.1.3 Nye tensor

The lattice incompatibility needs to be full-filled by dislocations that are called geometrically-necessary dislocations unless there is a discontinuity like a crack or void.

Nye defined the dislocation tensor as the dislocations that pierce through an arbitrary area normal contribute as much as their projected Burgers vector [12] as in Eq. (8.19):

$$\mathbf{B}_{net} = \int_S \left(\sum_a \rho^a_{GND} b^a \mathbf{s}^a \otimes \mathbf{t}^a \right) \cdot \mathbf{r} \, \mathrm{d}S \tag{8.19}$$

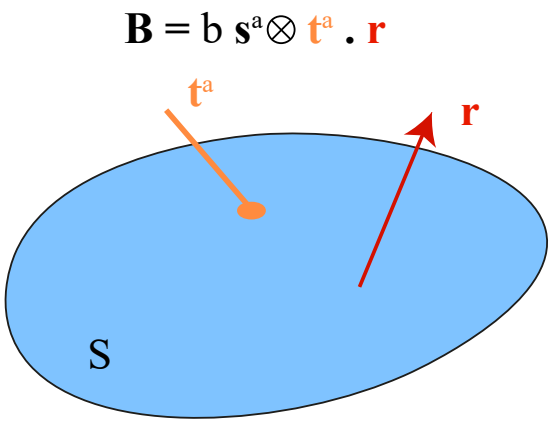

Figure 4: Sketch to explain physical meaning of dislocation tensor.

Fig. 4 shows the contribution of any dislocation to the incompatibility based on its line direction $\mathbf{t}^a$ and area normal at which Burgers circuit is constructed.

Setting the two equations; Eq. (8.5) and Eq. (8.19) equal to each other gives:

$$\mathbf{B}_{net} = -\int_S (\nabla \times \mathbf{F}_p)^T \cdot \mathbf{r} \mathrm{d}S = \int_S \left(\sum_a \rho^a_{GND} b^a \mathbf{s}^a \otimes \mathbf{t}^a \right) \cdot \mathbf{r} \, \mathrm{d}S \tag{8.20}$$

Cancelling out the integral expressions on both sides gives the overall incompatibility measure as:

$$\Lambda = -(\nabla \times \mathbf{F}_p)^T = \sum_a \rho^a_{GND} b^a \mathbf{s}^a \otimes \mathbf{t}^a \tag{8.21}$$

Therefore, Nye tensor for incompatibility becomes:

$$\Lambda = \sum_a \rho^a_{GND} b^a \mathbf{s}^a \otimes \mathbf{t}^a \tag{8.22}$$

Similarly, the incompatibility measure using the curl becomes:

$$\Lambda = -(\nabla \times \mathbf{F}_p)^T \tag{8.23}$$

Note that the incompatibility tensor can be written as the sum of dislocation families; screws (their line direction being along slip direction, $\mathbf{s}^a$) and edges (their line direction being along the tangent direction $\mathbf{t}^a$):

$$\Lambda = \sum_a \rho^a_{GND,e} b^a \mathbf{s}^a \otimes \mathbf{t}^a + \rho^a_{GND,s} b^a \mathbf{s}^a \otimes \mathbf{s}^a \tag{8.24}$$

8.1.4 Lattice curvature

Curvature tensor is computed using the incompatibility according to Eq. (8.25):

$$\kappa_{ij} = -\Lambda_{ji} + \frac{1}{2}\,\delta_{ij}\,\Lambda_{kk} \tag{8.25}$$

This equation ignores elastic strain gradients and computes curvature using total lattice incompatibility obtained by rotations [13].

After the calculation of incompatibility, either in incremental or total form, curvature is computed using the total incompatibility and stored as a state variable in the code.

8.1.5 Small strains

Consider small strains ($\|\gamma\| \ll 1$). The plastic part of the deformation gradient reduces to:

$$\mathbf{F}_p = \sum_a \gamma^a\,\mathbf{s}^a \otimes \mathbf{n}^a + \mathbf{I} \tag{8.26}$$

Substitute the simplified plastic deformation gradient expression to incompatibility with the curl:

$$\Lambda = -\left(\nabla \times \mathbf{F}_p\right) = -\left[\nabla \times \left(\sum_a \gamma^a\,\mathbf{s}^a \otimes \mathbf{n}^a + \mathbf{I}\right)^T\right]^T \tag{8.27}$$

$\nabla \times \mathbf{I}$ is zero because gradient of a constant tensor simply vanishes giving:

$$\Lambda = -\left(\nabla \times \sum_a \gamma^a\,\mathbf{s}^a \otimes \mathbf{n}^a\right)^T \tag{8.28}$$

The summation can be taken out the parenthesis since it is independent of the curl operation giving:

$$\Lambda = -\sum_a \left[\nabla \times \left(\gamma^a\,\mathbf{s}^a \otimes \mathbf{n}^a\right)\right]^T \tag{8.29}$$

The gradient operation can be simplified taking directional derivatives along slip direction, slip plane normal and line (tangent) direction, respectively. These derivatives are indicated with the comma symbols with the following expressions:

$$\nabla\gamma^a = \gamma^a_{,\mathbf{s}^a}\mathbf{s}^a + \gamma^a_{,\mathbf{n}^a}\mathbf{n}^a + \gamma^a_{,\mathbf{t}^a}\mathbf{t}^a \tag{8.30}$$

The same definition for the calculation of a curl of the second rank tensor is used here[2]. The curl applies to the rightmost vector component of the dyadic and the result of the cross-product is assigned to the leftmost vector component of the dyadic. Substituting these directional derivatives to compute the curl expression:

$$\Lambda = -\sum_a \left(\gamma^a_{,\mathbf{s}^a}\mathbf{s}^a \times \mathbf{n}^a \otimes \mathbf{s}^a + \gamma^a_{,\mathbf{n}^a}\mathbf{n}^a \times \mathbf{n}^a \otimes \mathbf{s}^a + \gamma^a_{,\mathbf{t}^a}\mathbf{t}^a \times \mathbf{n}^a \otimes \mathbf{s}^a\right)^T \tag{8.31}$$

Note that the second expression vanishes ($\mathbf{n}^a \times \mathbf{n}^a = \mathbf{0}$) and taking the cross-products simplifies the overall expression to:

$$\Lambda = -\sum_a \left(\gamma^a_{,\mathbf{s}^a}\mathbf{t}^a \otimes \mathbf{s}^a - \gamma^a_{,\mathbf{t}^a}\mathbf{s}^a \otimes \mathbf{s}^a\right)^T \tag{8.32}$$

Further simplification with the signs:

$$\Lambda = \sum_a \left(\gamma^a_{,\mathbf{t}^a}\mathbf{s}^a \otimes \mathbf{s}^a - \gamma^a_{,\mathbf{s}^a}\mathbf{t}^a \otimes \mathbf{s}^a\right)^T \tag{8.33}$$

[2]Note that there are mainly three different types of curl [14]. In this reference the curl of a second-rank tensor, $\mathbf{B}$, is calculated as follows: $\mathbf{A} = \nabla \times \mathbf{B}$ in index notation giving: $A_{ij} = \varepsilon_{irs} B_{js,r}$.

Taking the transpose:

$$\Lambda = \sum_a \gamma^a_{,\mathbf{t}^a} \mathbf{s}^a \otimes \mathbf{s}^a - \gamma^a_{,\mathbf{s}^a} \mathbf{s}^a \otimes \mathbf{t}^a \tag{8.34}$$

This equation is equal to the dislocation tensor given considering the two families of dislocations as in Eq. (8.24) giving:

$$\Lambda = \sum_a \gamma^a_{,\mathbf{t}^a} \mathbf{s}^a \otimes \mathbf{s}^a - \gamma^a_{,\mathbf{s}^a} \mathbf{s}^a \otimes \mathbf{t}^a = \sum_a \rho^a_{GND,e} b^a \mathbf{s}^a \otimes \mathbf{t}^a + \rho^a_{GND,s} b^a \mathbf{s}^a \otimes \mathbf{s}^a \tag{8.35}$$

Therefore, the individual dislocation densities per slip system can computed as:

$$b^a \rho^a_{GND,e} = -\gamma^a_{,\mathbf{s}^a} \tag{8.36}$$

$$b^a \rho^a_{GND,s} = \gamma^a_{,\mathbf{t}^a} \tag{8.37}$$

Directional derivatives can also be written as:

$$\gamma^a_{,\mathbf{s}^a} = \nabla \gamma^a \cdot \mathbf{s}^a \tag{8.38}$$

$$\gamma^a_{,\mathbf{t}^a} = \nabla \gamma^a \cdot \mathbf{t}^a \tag{8.39}$$

Therefore, the edge dislocations become the gradient of slip along the slip direction (negative sign is due to the dislocation convention):

$$\rho^a_{GND,e} = -\frac{1}{b^a} \nabla \gamma^a \cdot \mathbf{s}^a \tag{8.40}$$

While, the screw dislocations become the gradient of slip along the transverse direction:

$$\rho^a_{GND,s} = \frac{1}{b^a} \nabla \gamma^a \cdot \mathbf{t}^a \tag{8.41}$$

8.1.6 Rate form

The rate form has advantage to respond sudden changes in the strain or the strain path causing less changes. In addition, this formulation uses the curl of a vector instead of using the curl second rank tensor which has different forms in the literature to avoid confusion [14].

The rate form the incompatibility is obtained by simply taking the time derivative of the expression in Eq. (8.23) giving:

$$\dot{\Lambda} = -\left(\nabla \times \dot{\mathbf{F}}_p\right)^T \tag{8.42}$$

Note that $\dot{\mathbf{F}}_p$ can be computed in terms of the velocity gradient as:

$$\dot{\mathbf{F}}_p = \mathbf{L}_p \mathbf{F}_p \tag{8.43}$$

The plastic velocity gradient:

$$\mathbf{L}_p = \sum_a \dot{\gamma}^a \mathbf{s}^a \otimes \mathbf{n}^a \tag{8.44}$$

Substituting the $\mathbf{L}_p$ to the rate of change of plastic deformation gradient:

$$\dot{\mathbf{F}}_p = \left(\sum_a \dot{\gamma}^a \mathbf{s}^a \otimes \mathbf{n}^a\right) \mathbf{F}_p \tag{8.45}$$

The multiplication can be placed inside the summation as:

$$\dot{\mathbf{F}}_p = \sum_a \left(\dot{\gamma}^a \mathbf{s}^a \otimes \mathbf{n}^a \cdot \mathbf{F}_p\right) \tag{8.46}$$

Refer to the right most term as another vector to avoid confusion:

$$\mathbf{x}^a = \dot{\gamma}^a \mathbf{n}^a \cdot \mathbf{F}_p \tag{8.47}$$

Again, substituting the above expression to the incompatibility rate equation:

$$\dot{\Lambda} = -\left\{\nabla \times \left(\sum_a \mathbf{s}^a \otimes \mathbf{x}^a\right)\right\}^T \tag{8.48}$$

This expression is simply taking the curl of a second rank tensor as shown earlier:

$$\dot{\Lambda} = -\left[\sum_a (\nabla \times \mathbf{x}^a) \otimes \mathbf{s}^a\right]^T \tag{8.49}$$

The summation can be taken out the operations giving an incompatibility rate measure per slip system:

$$\dot{\Lambda}^a = -[(\nabla \times \mathbf{x}^a) \otimes \mathbf{s}^a]^T \tag{8.50}$$

Substituting back the expression for the simplified vector $\mathbf{x}^a$:

$$\dot{\Lambda}^a = -[(\nabla \times \mathbf{n}^a \mathbf{F}_p \dot{\gamma}^a) \otimes \mathbf{s}^a]^T \tag{8.51}$$

Therefore, the outermost transpose can be taken to give:

$$\dot{\Lambda}^a = -\mathbf{s}^a \otimes (\nabla \times \mathbf{n}^a \mathbf{F}_p \dot{\gamma}^a) \tag{8.52}$$

Using Eq. (8.22), the very same incompatibility rate needs to be satisfied using Nye's dislocation tensor considering different components of GNDs including edge dislocation density along the tangential direction $\dot{\rho}_{GND,et}$, edge dislocation density along the slip plane normal, $\dot{\rho}_{GND,en}$, and screw dislocations, $\dot{\rho}_{GND,s}$. Equating compatibility rate measures we obtain:

$$\dot{\Lambda}^a = b^a \dot{\rho}^a_{GND,et} \mathbf{s}^a \otimes \mathbf{t}^a + b^a \dot{\rho}^a_{GND,en} \mathbf{s}^a \otimes \mathbf{n}^a + b^a \dot{\rho}^a_{GND,s} \mathbf{s}^a \otimes \mathbf{s}^a \tag{8.53}$$

Equating the incompatibility rate measures in Eq. (8.52) and (8.53) gives:

$$\begin{aligned} \dot{\Lambda}^a &= -\mathbf{s}^a \otimes \nabla \times \dot{\gamma}^a \mathbf{n}^a \mathbf{F}_p \\ = b^a \dot{\rho}^a_{GND,et} \mathbf{s}^a \otimes \mathbf{t}^a &+ b^a \dot{\rho}^a_{GND,en} \mathbf{s}^a \otimes \mathbf{n}^a + b^a \dot{\rho}^a_{GND,s} \mathbf{s}^a \otimes \mathbf{s}^a \end{aligned} \tag{8.54}$$

Note that the slip direction vector can be cancelled out on both sides of the equations to give a simplified expression:

$$-\nabla \times \dot{\gamma}^a \mathbf{n}^a \mathbf{F}_p = b^a \dot{\rho}^a_{GND,et} \mathbf{t}^a + b^a \dot{\rho}^a_{GND,en} \mathbf{n}^a + b^a \dot{\rho}^a_{GND,s} \mathbf{s}^a \tag{8.55}$$

Simply using the vector projections and re-arranging terms, three equations for different families of dislocations can be computed:

$$\dot{\rho}^a_{GND,et} = -\frac{1}{b^a} (\nabla \times \dot{\gamma}^a \mathbf{n}^a \mathbf{F}_p) \cdot \mathbf{t}^a \tag{8.56}$$

$$\dot{\rho}^a_{GND,en} = -\frac{1}{b^a} (\nabla \times \dot{\gamma}^a \mathbf{n}^a \mathbf{F}_p) \cdot \mathbf{n}^a \tag{8.57}$$

$$\dot{\rho}^a_{GND,s} = -\frac{1}{b^a} (\nabla \times \dot{\gamma}^a \mathbf{n}^a \mathbf{F}_p) \cdot \mathbf{s}^a \tag{8.58}$$

The formulations explained here can also be found in the reference [10]. Several different references use exactly the same formulation to compute GNDs [7, 15, 16].

8.2 GND calculation methods (options)

Five different strain gradient calculation options available within the code excluding no GND calculation option. These are described in the following:

8.2.1 No GNDs (gndmodel=0)

GNDs are not computed if this option is selected.

8.2.2 Curl of $\mathbf{F}_p$ followed by rank-deficit inversion (gndmodel=1)

This was the existing GND model that is explained in detail in the reference . The only difference is transpose of the overall expression is taken in order to

The incompatibility measure is given as (Note that it is not in its rate form):

$$\boldsymbol{\Lambda} = -\left(\nabla \times \mathbf{F}_p\right)^T \tag{8.59}$$

In index notation using the same definition for the curl of the second rank tensor we find :

$$\boldsymbol{\Lambda} = -\left[\boldsymbol{\varepsilon}_{ijk}\left(\mathbf{F}_p\right)_{lj,i}\hat{\mathbf{e}}_k \otimes \hat{\mathbf{e}}_l\right]^T \tag{8.60}$$

Taking the transpose gives:

$$\Lambda_{lk} = -\boldsymbol{\varepsilon}_{ijk}\left(\mathbf{F}_p\right)_{lj,i}\hat{\mathbf{e}}_l \otimes \hat{\mathbf{e}}_k \tag{8.61}$$

Or more simply:

$$\Lambda_{lk} = -\boldsymbol{\varepsilon}_{ijk}\left(\mathbf{F}_p\right)_{lj,i} \tag{8.62}$$

Check the curl as used in [17]:

The curl without the negative sign is used in the reference [17]:

$$\left(\Lambda^*\right)^T = \nabla \times \mathbf{F}_p \tag{8.63}$$

In index notation it is given as on page 79 of the reference [17] as:

$$\Lambda^*_{lk} = \boldsymbol{\varepsilon}_{ijk}\left(\mathbf{F}_p\right)_{lj,i} \tag{8.64}$$

We have found the the incompatibility in index notation is given as in Eq. (8.62) which is checked for consistency using the small strain case:

$$\Lambda_{lk} = -\boldsymbol{\varepsilon}_{ijk}\left(\mathbf{F}_p\right)_{lj,i} \tag{8.65}$$

Therefore, the two expressions are not the same, indeed it is equal to the negative and transpose of it:

$$\boldsymbol{\Lambda} = -\boldsymbol{\Lambda}^* \tag{8.66}$$

GND density is computed using the equation in the reference [13]:

$$[\mathbf{A}]\left\{\rho_{GND}\right\} = \{\Lambda\} \tag{8.67}$$

B is computed from the Nye's tensor $\boldsymbol{\Lambda}$ as:

$$\left\{\rho_{GND}\right\} = [\mathbf{B}]\{\Lambda\} \tag{8.68}$$

where **B** is obtained using inversion, but the inversion is rank deficit giving large densities:

$$\mathbf{B} = \mathbf{A}^T \left(\mathbf{A}\mathbf{A}^T\right)^{-1} \tag{8.69}$$

Instead the B-matrix available in literature can be used however, it is only available for FCC materials. An example **B** is shown for FCC type materials [13]:

$$[\mathbf{B}] = \begin{bmatrix}
a & 7c & -13c & -7c & -a & 13c & c & -c & 0 \\
-a & 13c & -7c & -c & 0 & c & 7c & -13c & a \\
0 & c & -c & -13c & a & 7c & 13c & -7c & -a \\
a & -7c & 13c & 7c & -a & 13c & -c & -c & 0 \\
-a & -13c & 7c & c & 0 & c & -7c & -13c & a \\
0 & -c & c & 13c & a & 7c & -13c & -7c & -a \\
a & -7c & -13c & 7c & -a & -13c & c & c & 0 \\
-a & -13c & -7c & c & 0 & -c & 7c & 13c & a \\
0 & -c & -c & 13c & a & -7c & 13c & 7c & -a \\
a & 7c & 13c & -7c & -a & -13c & -c & c & 0 \\
-a & 13c & 7c & -c & 0 & -c & -7c & 13c & a^* \\
0 & c & c & -13c & a & -7c & -13c & 7c & -a \\
5d & e & 0 & e & 5d & 0 & 0 & 0 & -d \\
5d & 0 & e & 0 & -d & 0 & e & 0 & 5d \\
-d & 0 & 0 & 0 & 5d & e & 0 & e & 5d \\
5d & -e & 0 & -e & 5d & 0 & 0 & 0 & -d \\
5d & 0 & -e & 0 & -d & 0 & -e & 0 & 5d \\
-d & 0 & 0 & 0 & 5d & -e & 0 & -e & 5d
\end{bmatrix} \tag{8.70}$$

where $a = \sqrt{3}/9$, $c = \sqrt{3}/84$, $d = 1/18$, $e = 3/14$ as in the reference [13].

8.2.3 Curl of $\mathbf{F}_p$ followed by L2 minimization (gndmodel=2) using KKT solution

The incompatibility calculation procedure is the same as in gndmodel-1 using curl of Fp:

$$\Lambda_{lk} = \varepsilon_{jik} \left(\mathbf{F}_p\right)_{lj,i} \tag{8.71}$$

The only difference is in the calculation of GNDs. In this case we used Karush-Kuhn-Tucker (KKT) condition to solve for the L2 minimization.

The L2 functional is defined in the reference as C which is a function of GND density, ρ, and penalty factor of the Lagrange multipliers, y:

$$C(\rho, y) = \rho^T \rho + y^T \left(\mathbf{A}\rho - \Lambda\right) \tag{8.72}$$

KKT optimality criteria are:

$$\frac{\partial C(\rho, y)}{\partial \rho} = 0 \tag{8.73}$$

$$\frac{\partial C(\rho, y)}{\partial y} = 0 \tag{8.74}$$

giving two equations:

$$2\rho + y^T \mathbf{A} = 0 \tag{8.75}$$

$$\mathbf{A}\rho - \Lambda = 0 \tag{8.76}$$

In matrix form, simply noting $y^T \mathbf{A} = \mathbf{A}^T y$

$$\begin{bmatrix} 2\mathbf{I} & \mathbf{A}^T \\ \mathbf{A} & \mathbf{0} \end{bmatrix} \begin{Bmatrix} \rho \\ y \end{Bmatrix} = \begin{Bmatrix} 0 \\ \Lambda \end{Bmatrix} \tag{8.77}$$

Therefore, the solution for the GND density is obtained by simply inverting this matrix.
This has two conditions for invertibility:

1. The stacked matrix $\begin{bmatrix} \mathbf{I} \\ \mathbf{A} \end{bmatrix}$ should have linearly independent columns.
2. The matrix $\mathbf{A}$ should have linearly independent rows

The rank of the overall matrix is checked for FCC case, and it had full-rank.

8.2.4 Curl of $\mathbf{F}_p$ followed by L2 minimization (gndmodel=3) SVD solution

The calculation of incompatibility is the same as in gndmodel-1 and gndmodel-2.

$$\Lambda_{lk} = \varepsilon_{jik} \left(\mathbf{F}_p\right)_{lj,i} \tag{8.78}$$

The only difference is in the calculation of $[\mathbf{B}]$ matrix. The non-active slip systems that have a total slip less than $10^{-10}$are eliminated from the Nye tensor. The solution is obtained by singular value decomposition (SVD) method to invert the $[\mathbf{B}]^T[\mathbf{B}]$ matrix to solve for GND densities.

8.2.5 Rate form (curl of $\mathbf{n}^a \mathbf{F}_p$) with direct projection (gndmodel=4)

Curl of $\mathbf{n}^a \mathbf{F}_p$ is directly projected to slip systems to the slip systems.

Rate of change of incompatibility measure is, which is a vector $\dot{\lambda}^a$:

$$\dot{\lambda}^a = -\nabla \times (\dot{\gamma}^a \mathbf{n}^a \mathbf{F}_p) \tag{8.79}$$

GND density rates are obtained by projections to the slip systems:

$$\dot{\rho}^a_{GND,et} = \dot{\lambda}^a \cdot \mathbf{t}^a \tag{8.80}$$

$$\dot{\rho}^a_{GND,en} = \dot{\lambda}^a \cdot \mathbf{n}^a \tag{8.81}$$

$$\dot{\rho}^a_{GND,s} = \dot{\lambda}^a \cdot \mathbf{s}^a \tag{8.82}$$

8.2.6 Norm of the rate form (gndmodel=5)

GNDs are computed by the norm of the curl as a scalar quantity:

$$\dot{\rho}_{GND} = \|\nabla \times (\dot{\gamma}^a \mathbf{n}^a \mathbf{F}_p)\| \tag{8.83}$$

8.2.7 Slip gradients (gndmodel=6)

The GNDs are computed directly from slip gradients assuming small strains:

$$\dot{\rho}^a_{GND,e} = -\nabla \dot{\gamma}^a \cdot \mathbf{s}^a \tag{8.84}$$

$$\dot{\rho}^a_{GND,s} = \nabla \dot{\gamma}^a \cdot \mathbf{t}^a \tag{8.85}$$

9 Element library

DBF code can use various element types which is important for GND calculation.

Some important remarks about element types are as follows:

- The element names have the same as in ABAQUS library (i.e. C3D8 is defined in DBF-code as C3D8.)
- The element types shall be the same and single type only within the mesh
- The number of elements must be prescribed in the userinputs.f
- ABAQUS uses g, h, r as the identifies for the isoparametric coordinates for 3D, and g, h for 2D.

9.1 2D elements

2D elements are distinguished as plane stress or plane strain. The same interpolation functions are used for both cases.

9.1.1 CPS4/CPE4

4-noded linear quadrilateral elements

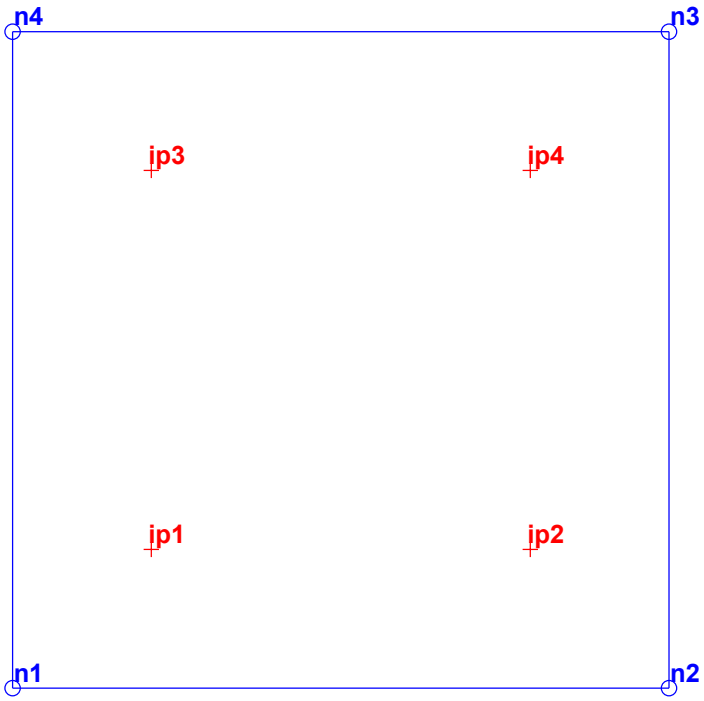

Figure 5: Node (n) and integration point (ip) numbering.

$$N_1 = \frac{1}{4}(1-g)(1-h) \tag{9.1}$$

$$N_2 = \frac{1}{4}(1+g)(1-h) \tag{9.2}$$

$$N_3 = \frac{1}{4}(1+g)(1+h) \tag{9.3}$$

$$N_4 = \frac{1}{4}(1-g)(1+h) \tag{9.4}$$

$$\tag{9.5}$$

9.1.2 CPS6/CPE6

6-node quadratic triangular elements

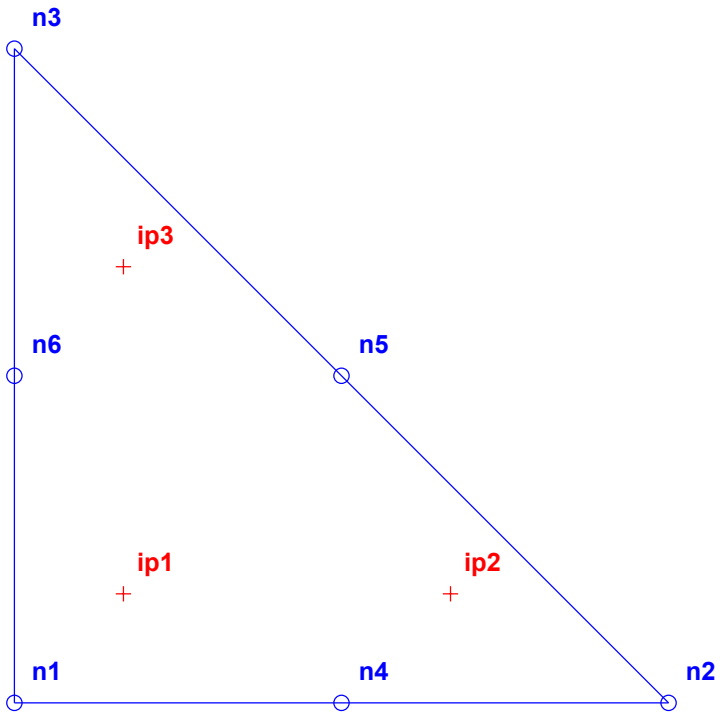

Figure 6: Node (n) and integration point (ip) numbering.

$$N_1 = 2(\frac{1}{2} - g - h)(1 - g - h) \tag{9.6}$$

$$N_2 = 2g(g - \frac{1}{2}) \tag{9.7}$$

$$N_3 = 2h(h - \frac{1}{2}) \tag{9.8}$$

$$N_4 = 4g(1 - g - h) \tag{9.9}$$

$$N_5 = 4gh \tag{9.10}$$

$$N_6 = 4h(1 - g - h) \tag{9.11}$$

9.1.3 CPS8/CPE8

8-noded quadrilateral elements

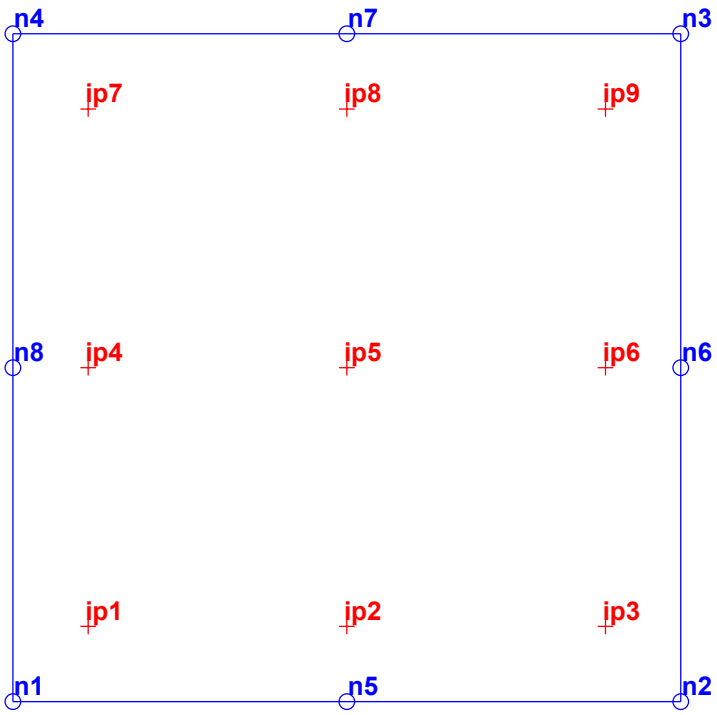

Figure 7: Node (n) and integration point (ip) numbering.

$$N_1 = -\frac{1}{4}(1-g)(1-h)(1+g+h) \tag{9.12}$$

$$N_2 = -\frac{1}{4}(1+g)(1-h)(1-g+h) \tag{9.13}$$

$$N_3 = -\frac{1}{4}(1+g)(1+h)(1-g-h) \tag{9.14}$$

$$N_4 = -\frac{1}{4}(1-g)(1+h)(1+g-h) \tag{9.15}$$

$$N_5 = \frac{1}{2}(1-g)(1+g)(1-h) \tag{9.16}$$

$$N_6 = \frac{1}{2}(1-h)(1+h)(1+g) \tag{9.17}$$

$$N_7 = \frac{1}{2}(1-g)(1+g)(1+h) \tag{9.18}$$

$$N_8 = \frac{1}{2}(1-h)(1+h)(1-g) \tag{9.19}$$

$$\tag{9.20}$$

9.1.4 CPS8R/CPE8R = CPS4/CPE4

8-node quadrilateral with reduced integration

For this element type, the same node numbering and interpolation functions are used as for CPS4/CPE4 type elements.

9.2 3D elements

9.2.1 C3D8

8-node linear solid brick elements

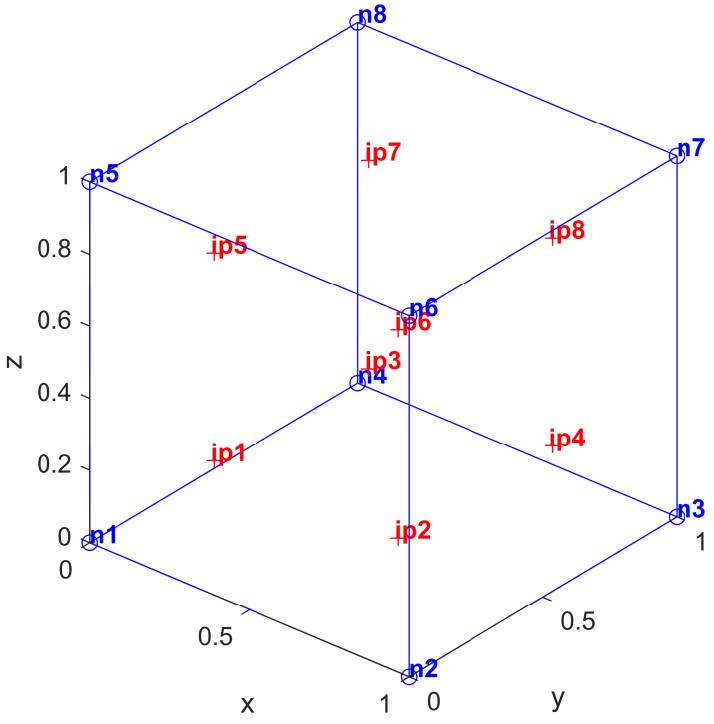

Figure 8: Node (n) and integration point (ip) numbering.

$$N_1 = \frac{1}{8}(1-g)(1-h)(1-r) \tag{9.21}$$

$$N_2 = \frac{1}{8}(1+g)(1-h)(1-r) \tag{9.22}$$

$$N_3 = \frac{1}{8}(1+g)(1+h)(1-r) \tag{9.23}$$

$$N_4 = \frac{1}{8}(1-g)(1+h)(1-r) \tag{9.24}$$

$$N_5 = \frac{1}{8}(1-g)(1-h)(1+r) \tag{9.25}$$

$$N_6 = \frac{1}{8}(1+g)(1-h)(1+r) \tag{9.26}$$

$$N_7 = \frac{1}{8}(1+g)(1+h)(1+r) \tag{9.27}$$

$$N_8 = \frac{1}{8}(1-g)(1+h)(1+r) \tag{9.28}$$

$$\tag{9.29}$$

9.2.2 C3D10

10-node quadratic tetrahedron elements

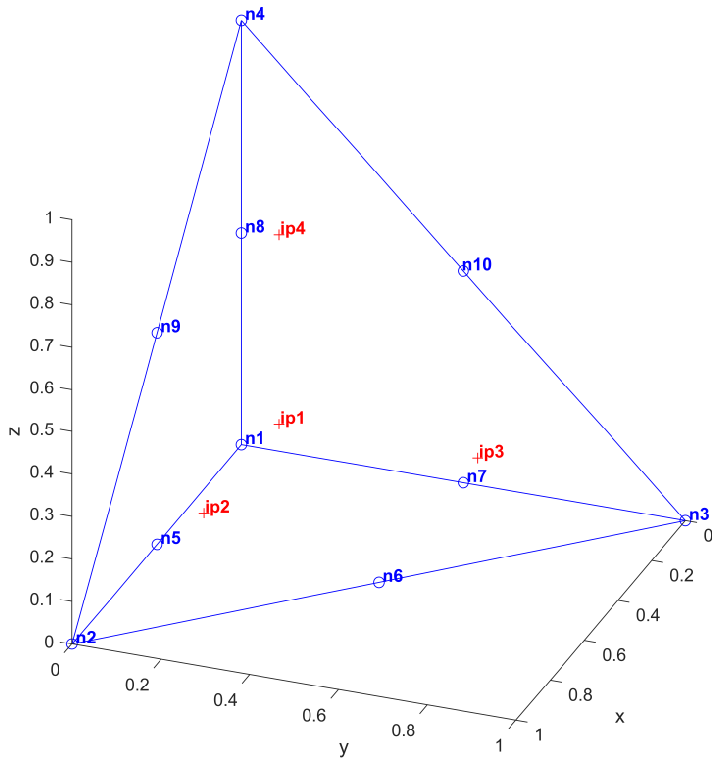

Figure 9: Node (n) and integration point (ip) numbering.

$$N_1 = (2(1-g-h-r)-1)(1-g-h-r) \tag{9.30}$$
$$N_2 = (2g-1)g \tag{9.31}$$
$$N_3 = (2h-1)h \tag{9.32}$$
$$N_4 = (2r-1)r \tag{9.33}$$
$$N_5 = 4(1-g-h-r)g \tag{9.34}$$
$$N_6 = 4gh \tag{9.35}$$
$$N_7 = 4(1-g-h-r)h \tag{9.36}$$
$$N_8 = 4(1-g-h-r)r \tag{9.37}$$
$$N_9 = 4gr \tag{9.38}$$
$$N_{10} = 4hr \tag{9.39}$$
$$\tag{9.40}$$

9.2.3 C3D15

15-node quadratic wedge elements

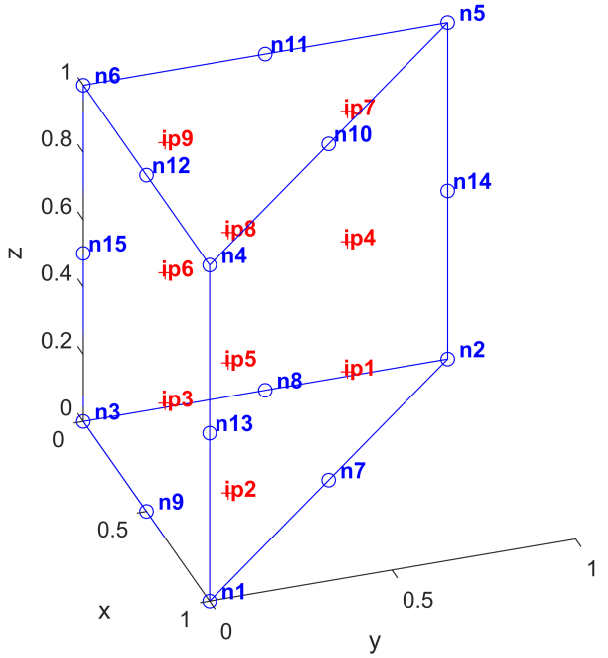

Figure 10: Node (n) and integration point (ip) numbering.

$$N_1 = \frac{1}{2}\left[(1-g-h)\left(2\left(1-g-h\right)-1\right)(1-r)-(1-g-h)\left(1-r^2\right)\right] \tag{9.41}$$

$$N_2 = \frac{1}{2}\left[g\left(2g-1\right)(1-r)-g\left(1-r^2\right)\right] \tag{9.42}$$

$$N_3 = \frac{1}{2}\left[h\left(2h-1\right)(1-r)-h\left(1-r^2\right)\right] \tag{9.43}$$

$$N_4 = \frac{1}{2}\left[(1-g-h)\left(2\left(1-g-h\right)-1\right)(1+r)-(1-g-h)\left(1-r^2\right)\right] \tag{9.44}$$

$$N_5 = \frac{1}{2}\left[g\left(2g-1\right)(1+r)-g\left(1-r^2\right)\right] \tag{9.45}$$

$$N_6 = \frac{1}{2}\left[h\left(2h-1\right)(1+r)-h\left(1-r^2\right)\right] \tag{9.46}$$

$$N_7 = 2\left(1-g-h\right)g\left(1-r\right) \tag{9.47}$$

$$N_8 = 2ghr\left(1-r\right) \tag{9.48}$$

$$N_9 = 2h\left(1-g-h\right)\left(1-r\right) \tag{9.49}$$

$$N_{10} = 2\left(1-g-h\right)g\left(1+r\right) \tag{9.50}$$

$$N_{11} = 2ghr\left(1+r\right) \tag{9.51}$$

$$N_{12} = 2h\left(1-g-h\right)\left(1+r\right) \tag{9.52}$$

$$N_{13} = \left(1-g-h\right)\left(1-r^2\right) \tag{9.53}$$

$$N_{14} = g\left(1-r^2\right) \tag{9.54}$$

$$N_{15} = h\left(1-r^2\right) \tag{9.55}$$

$$\tag{9.56}$$

9.2.4 C3D20

20-node quadratic solid brick elements

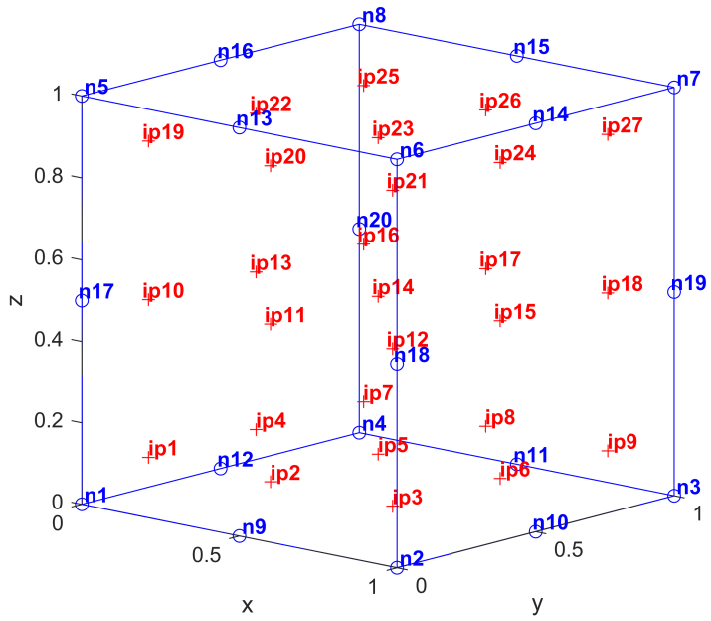

Figure 11: Node (n) and integration point (ip) numbering.

$$N_1 = (g/8-1/8)(h-1)(r-1)(g+h+r+2) \tag{9.57}$$
$$N_2 = -(g/8+1/8)(h-1)(r-1)(h-g+r+2) \tag{9.58}$$
$$N_3 = -(g/8+1/8)(h+1)(r-1)(g+h-r-2) \tag{9.59}$$
$$N_4 = -(g/8-1/8)(h+1)(r-1)(g-h+r+2) \tag{9.60}$$
$$N_5 = -(g/8-1/8)(h-1)(r+1)(g+h-r+2) \tag{9.61}$$
$$N_6 = -(g/8+1/8)(h-1)(r+1)(g-h+r-2) \tag{9.62}$$
$$N_7 = (g/8+1/8)(h+1)(r+1)(g+h+r-2) \tag{9.63}$$
$$N_8 = (g/8-1/8)(h+1)(r+1)(g-h-r+2) \tag{9.64}$$
$$N_9 = -(g/4-1/4)(g+1)(h-1)(r-1) \tag{9.65}$$
$$N_{10} = (h/4-1/4)(g+1)(h+1)(r-1) \tag{9.66}$$
$$N_{11} = (g/4-1/4)(g+1)(h+1)(r-1) \tag{9.67}$$
$$N_{12} = -(h/4-1/4)(g-1)(h+1)(r-1) \tag{9.68}$$
$$N_{13} = (g/4-1/4)(g+1)(h-1)(r+1) \tag{9.69}$$
$$N_{14} = -(h/4-1/4)(g+1)(h+1)(r+1) \tag{9.70}$$
$$N_{15} = -(g/4-1/4)(g+1)(h+1)(r+1) \tag{9.71}$$
$$N_{16} = (h/4-1/4)(g-1)(h+1)(r+1) \tag{9.72}$$
$$N_{17} = -(r/4-1/4)(g-1)(h-1)(r+1) \tag{9.73}$$
$$N_{18} = (r/4-1/4)(g+1)(h-1)(r+1) \tag{9.74}$$
$$N_{19} = -(r/4-1/4)(g+1)(h+1)(r+1) \tag{9.75}$$
$$N_{20} = (r/4-1/4)(g-1)(h+1)(r+1) \tag{9.76}$$
$$\tag{9.77}$$

References

[1] Dan Zhao, Yi-Guo Zhu, Ping Hu, and Wan-Xi Zhang. A new integration algorithm for finite deformation of thermo-elasto-viscoplastic single crystals. *Acta Mechanica Sinica*, 29(5):709–717, 2013.

[2] William D Musinski and David L McDowell. On the eigenstrain application of shot-peened residual stresses within a crystal plasticity framework: Application to ni-base superalloy specimens. *International Journal of Mechanical Sciences*, 100:195–208, 2015.

[3] Ping Hu, Yang Liu, Yiguo Zhu, and Liang Ying. Crystal plasticity extended models based on thermal mechanism and damage functions: Application to multiscale modeling of aluminum alloy tensile behavior. *International Journal of Plasticity*, 86:1–25, 2016.

[4] Cedric Nicholas Reid. *Deformation geometry for materials scientists: international series on materials science and technology*, volume 11. Elsevier, 2016.

[5] R Hill and JR0254 Rice. Constitutive analysis of elastic-plastic crystals at arbitrary strain. *Journal of the Mechanics and Physics of Solids*, 20(6):401–413, 1972.

[6] Walter L Bond. The mathematics of the physical properties of crystals. *The Bell System Technical Journal*, 22(1):1–72, 1943.

[7] FPE Dunne, D Rugg, and A Walker. Lengthscale-dependent, elastically anisotropic, physically-based hcp crystal plasticity: Application to cold-dwell fatigue in ti alloys. *International Journal of Plasticity*, 23(6):1061–1083, 2007.

[8] Surya R Kalidindi, Curt A Bronkhorst, and Lallit Anand. Crystallographic texture evolution in bulk deformation processing of fcc metals. *Journal of the Mechanics and Physics of Solids*, 40(3):537–569, 1992.

[9] Chris Hardie, Rhys Thomas, Yang Liu, Philipp Frankel, and Fionn Dunne. Simulation of crystal plasticity in irradiated metals: A case study on zircaloy-4. *Acta Materialia*, 241:118361, 2022.

[10] Hong Dai. *Geometrically-necessary dislocation density in continuum plasticity theory, FEM implementation and applications*. PhD thesis, Massachusetts Institute of Technology, 1997.

[11] Paolo Cermelli and Morton E Gurtin. Geometrically necessary dislocations in viscoplastic single crystals and bicrystals undergoing small deformations. *International Journal of Solids and Structures*, 39(26):6281–6309, 2002.

[12] John F Nye. Some geometrical relations in dislocated crystals. *Acta metallurgica*, 1(2):153–162, 1953.

[13] A Arsenlis and DM Parks. Crystallographic aspects of geometrically-necessary and statistically-stored dislocation density. *Acta materialia*, 47(5):1597–1611, 1999.

[14] Suchandrima Das, Felix Hofmann, and Edmund Tarleton. Consistent determination of geometrically necessary dislocation density from simulations and experiments. *International Journal of Plasticity*, 109:18–42, 2018.

[15] EP Busso, FT Meissonnier, and NP O'dowd. Gradient-dependent deformation of two-phase single crystals. *Journal of the Mechanics and Physics of Solids*, 48(11):2333–2361, 2000.

[16] A Ma, F Roters, and D Raabe. A dislocation density based constitutive model for crystal plasticity fem including geometrically necessary dislocations. *Acta Materialia*, 54(8):2169–2179, 2006.

[17] Viacheslav Kuksenko, Steve Roberts, and Edmund Tarleton. The hardness and modulus of polycrystalline beryllium from nano-indentation. *International Journal of Plasticity*, 116:62–80, 2019.